

# Catalytic Turnover of [FeFe]-Hydrogenase Based on Single-Molecule Imaging

Christopher Madden,<sup>†</sup> Michael D. Vaughn,<sup>†</sup> Ismael Díez-Pérez,<sup>‡,§</sup> Katherine A. Brown,<sup>⊥</sup> Paul W. King,<sup>⊥</sup> Devens Gust,<sup>\*,†</sup> Ana L. Moore,<sup>\*,†</sup> and Thomas A. Moore<sup>\*,†</sup>

<sup>†</sup>Center for Bioenergy and Photosynthesis, Center for Bio-Inspired Solar Fuel Production and Department of Chemistry and Biochemistry, Arizona State University, Tempe, Arizona 85287-1604, United States

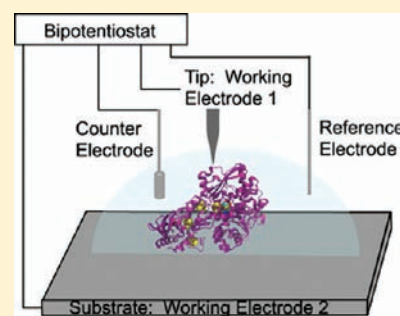
<sup>‡</sup>Center for Bioelectronics and Biosensors, Biodesign Institute and Department of Electrical Engineering, Arizona State University, Tempe, Arizona 85287, United States

<sup>§</sup>Department of Physical Chemistry, University of Barcelona, Barcelona, Spain 08028

<sup>⊥</sup>Biosciences Center, National Renewable Energy Laboratory, Golden, Colorado 80401, United States

 Supporting Information

**ABSTRACT:** Hydrogenases catalyze the interconversion of protons and hydrogen according to the reversible reaction:  $2\text{H}^+ + 2\text{e}^- \rightleftharpoons \text{H}_2$  while using only the earth-abundant metals nickel and/or iron for catalysis. Due to their high activity for proton reduction and the technological significance of the  $\text{H}^+/\text{H}_2$  half reaction, it is important to characterize the catalytic activity of [FeFe]-hydrogenases using both biochemical and electrochemical techniques. Following a detailed electrochemical and photoelectrochemical study of an [FeFe]-hydrogenase from *Clostridium acetobutylicum* (*CaHydA*), we now report electrochemical and single-molecule imaging studies carried out on a catalytically active hydrogenase preparation. The enzyme *CaHydA*, a homologue (70% identity) of the [FeFe]-hydrogenase from *Clostridium pasteurianum*, CpI, was adsorbed to a negatively charged, self-assembled monolayer (SAM) for investigation by electrochemical scanning tunneling microscopy (EC-STM) techniques and macroscopic electrochemical measurements. The EC-STM imaging revealed uniform surface coverage with sufficient stability to undergo repeated scanning with a STM tip as well as other electrochemical investigations. Cyclic voltammetry yielded a characteristic cathodic hydrogen production signal when the potential was scanned sufficiently negative. The direct observation of the single enzyme distribution on the Au-SAM surface coupled with macroscopic electrochemical measurements obtained from the same electrode allowed the evaluation of a turnover frequency (TOF) as a function of potential for single [FeFe]-hydrogenase molecules.



## INTRODUCTION

Hydrogenases are of growing interest due to their utilization of common metals at their active sites and ability to catalyze the  $2\text{H}^+ + 2\text{e}^- \rightleftharpoons \text{H}_2$  redox system under nearly activationless conditions, with concomitant energy storage or release.<sup>1–5</sup> They serve as models for catalysis of this most fundamental of redox reactions. Interest in the catalytic abilities of hydrogenases for hydrogen generation has led to various electrochemical studies<sup>6–9</sup> as well as photoelectrochemical hydrogen production studies.<sup>10</sup>

A typical [FeFe]-hydrogenase is *CaHydA*, a 65.4 kD protein with a highly conserved [6Fe-6S] catalytic H-cluster as well as three [4Fe-4S] and one [2Fe-2S] accessory clusters. The proximity of the distal [FeS] cluster to the exterior of the protein allows electrons to be transferred directly from an external redox partner, presumably through a chain of [FeS] clusters, to the H-cluster, where catalysis occurs and hydrogen is produced or oxidized.

Direct electrochemical measurement of catalytic currents on macroscopic electrodes as a function of applied potential has yielded valuable information.<sup>4</sup> The *CaHydA* [FeFe]-hydrogenase, as well as other [FeFe]-hydrogenases, reportedly show a

preference for proton reduction over hydrogen oxidation,<sup>5</sup> leading them to be investigated as a means of producing hydrogen. On the other hand, hydrogenases biased toward hydrogen oxidation could serve as catalysts in fuel cells.<sup>11</sup> The mechanism of bias in either hydrogen oxidation or proton reduction is not clear: electrochemical studies have shown that these catalysts appear to operate very near the prevailing thermodynamic potential of the  $\text{H}^+/\text{H}_2$  couple and therefore cannot differentially favor the reduction or oxidation.

Numerous electrochemical studies with both [NiFe]- and [FeFe]-hydrogenases have been performed at carbon electrodes,<sup>8,10,12–16</sup> while a handful have been performed on gold and modified gold electrodes.<sup>17,18</sup> Although most studies utilize hydrogenase adsorbed on an electrode as an ensemble average of orientations,<sup>19</sup> attempts have been made to specifically orient the protein on the electrode surface.<sup>20,21</sup> A suitably oriented molecule allows for better defined interfacial electron transfer<sup>22</sup> and the possibility of observing the largest current densities attainable

Received: August 15, 2011

Published: September 14, 2011

for a given system. Maximum current densities are necessary to observe maximum turnover, and the number of molecules participating in the reaction must be known in order to calculate the TOF. Previously, surface coverage of hydrogenases on electrodes was either estimated on the basis of the electroactive surface area of an electrode, or by inhibiting the enzyme to reveal nonturnover signals from redox cofactors inside the protein.<sup>23,24</sup> While the latter technique can be useful and has provided the first measurements of electroactive surface coverage, it has only been demonstrated in a limited number of cases with specific hydrogenases, most notably a [NiFe]-hydrogenase from *Allochrochromatium vinosum*.<sup>25</sup> Calculation of the electroactive surface coverage of enzyme enabled Armstrong et al., to calculate accurate TOFs for various hydrogenases.<sup>7,11</sup> One study has also shown that a [NiFe]-hydrogenase from *Thiocapsa roseopersicina* can be imaged with a scanning tunneling microscope in a Langmuir–Blodgett film; I–V curves of the protein film were reported.<sup>26</sup> The ability to measure redox processes of simple proteins through SAMs has also been investigated previously where one-electron oxidations and reductions were taking place.<sup>27</sup> More complicated, multielectron or catalytic processes have also been measured through SAMs. However those studies did not involve the use of single-molecule topographic techniques such as STM to determine surface concentrations.<sup>17,28</sup> Knowing the actual surface coverage on an atomically flat surface is crucial to accurately calculate the catalytic TOF, measured as a function of applied potential, per single adsorbed enzyme molecule.

The measurement of the maximum TOF of hydrogenase molecules is the most direct indication of catalytic prowess. Such a measurement requires accurate knowledge of the concentration of active protein and of substrates and products. However, performing this measurement in solution remains a formidable challenge because saturating concentrations for both substrates cannot be realized. Varying the substrate ( $H^+$ ) concentration as necessary to allow for a typical biochemical assay to determine the turnover of the hydrogenase is not possible because the protein is rendered inactive outside a narrow pH range.<sup>10,29,30</sup>

In this study, we investigate the enzymatic turnover of an [FeFe]-hydrogenase, CaHydA from *Clostridium acetobutylicum*, which is homologous (70% identity)<sup>31</sup> with the [FeFe]-hydrogenase from *C. pasteurianum*, Cpl, for which structural data exists.<sup>32,33</sup> The CaHydA was chosen for this study due to its high catalytic activity for hydrogen production and the relative ease of recombinant expression.<sup>31</sup> The enzyme was adsorbed onto a negatively charged SAM on a flat gold surface for investigation by electrochemical scanning tunneling microscopy (EC-STM) techniques and macroscopic electrochemical measurements. The EC-STM imaging allowed quantitative determination of the number of bound enzyme molecules. The bound enzymes were catalytically active, and cyclic voltammetry (CV) yielded a characteristic cathodic hydrogen production signal when the potential was scanned sufficiently negative. The quantitative determination of the enzyme distribution on the Au-SAM surface coupled with macroscopic electrochemical measurements obtained from the same electrode allowed the evaluation of a TOF as a function of potential for single [FeFe]-hydrogenase molecules.

## EXPERIMENTAL SECTION

Electrochemical scanning tunneling microscopy (EC-STM) studies were performed with a Pico-SPM (Agilent, AZ) using a Nanoscope E controller and a bipotentiostat (Agilent, AZ). Imaging experiments were

performed in a homemade Teflon cell using as a working electrode an atomically flat Au (111) substrate prepared by thermally evaporating  $\sim 130$  nm of gold (Alfa Aesar 99.999%) onto freshly cleaved mica surfaces under ultra high vacuum ( $\sim 2 \times 10^{-8}$  Torr). The STM tips were prepared by mechanically shearing Pt/Ir wire (80/20, 0.25 mm diameter) and coating the tips with Apiezon wax. All tips had  $<1$  pA leakage current, the tunneling current set point was 200–400 pA with a 10 nA/V current amplifier, and a 100 mV sample bias was typically applied. All Au (111) substrates were annealed with a hydrogen flame prior to use and subsequently immersed in ethanolic solutions of mercapto-carboxylic acids to form self-assembled monolayers (SAMs). The resulting SAMs were imaged without protein to ensure formation of the SAM and cleanliness of the surface. The CaHydA was subsequently adsorbed *in situ* to the monolayer with 0.1 M phosphate buffer, pH 7.0, as the supporting electrolyte and imaged in EC-STM mode to control substrate potential. All EC-STM images were recorded with a substrate potential of  $-400$  mV vs Ag/AgCl. Titration of protein to control surface coverage results in the adsorption of protein to the modified gold surface over the course of several minutes to a few hours to reach equilibrium.

The [FeFe]-hydrogenase CaHydA from *C. acetobutylicum* was purified and expressed in *Escherichia coli* and assayed for  $H_2$  evolution activity according to previously reported procedures.<sup>34</sup> Due to the extreme oxygen sensitivity of [FeFe]-hydrogenases,<sup>9,35,36</sup> all work was performed in an anaerobic chamber (Coy Laboratory Products) under strictly anaerobic conditions (2–3%  $H_2$ , bulk  $N_2$ ,  $<1$  ppm  $O_2$ ). Under anaerobic conditions and at ambient temperature ( $\sim 25$  °C), CaHydA is stable for several hours in the electrochemical STM setup with little or no observed loss in electrocatalytic activity. The specific activity units (U) are defined as 1  $\mu$ mol  $H_2$  produced  $min^{-1} mg^{-1}$  of enzyme from sodium dithionite reduced methyl viologen (7.5 mM) as an electron donor. This study used two separate CaHydA preparations with nominal solution-based specific activities for  $H_2$  production of 177 and 280  $U mg^{-1}$ , which correspond to TOFs of 192  $s^{-1}$  and 303  $s^{-1}$  respectively. All data were normalized to both the surface coverage of protein and the specific activity.

Cyclic voltammetry was performed with a CH Instruments 650C electrochemical workstation using a platinum wire counter electrode and either a silver wire quasi reference or a silver/silver chloride reference electrode. The Au (111) substrate modified with a carboxylate-terminated SAM was used as a working electrode. All CV was performed in the same EC-STM cell, with a geometric surface area of 0.283  $cm^2$ . The same sample was used for imaging by EC-STM inside an anaerobic chamber as well as anaerobic CV in a typical three-electrode configuration. All CVs were recorded in 0.1 M phosphate at pH 7.0 with a scan rate of 50 mV/s.

STM images were scrutinized by eye to estimate the number of proteins on the surface. Several 100 nm by 100 nm images from different areas of the electrode were analyzed, particles were counted, and an average coverage was obtained, which was then used to estimate the number of proteins on the geometric surface. Variation in surface coverage among images was  $<10\%$  for a given sample. To verify the methodology of counting individual particles in order to quantify enzymes on the electrode, two of the STM image-quantified samples were tested for iron content via a ferrozine iron binding assay adapted from previously reported procedures.<sup>37,38</sup> The quantity of iron determined by this procedure differed from that determined by counting the images by 20–50% underestimation, indicating that qualitatively the method of counting the images is valid. Due to the minute amounts of protein in the experiments, ( $\sim 10^{-12}$  mol of protein/ $cm^2$ ), the difficulty of recovering protein from surfaces, and detection limitations by UV–vis absorption measurements, data from the STM images alone were used to calculate a TOF in this report. Recovered samples were also analyzed by SDS-PAGE to confirm that the molecular weight of the

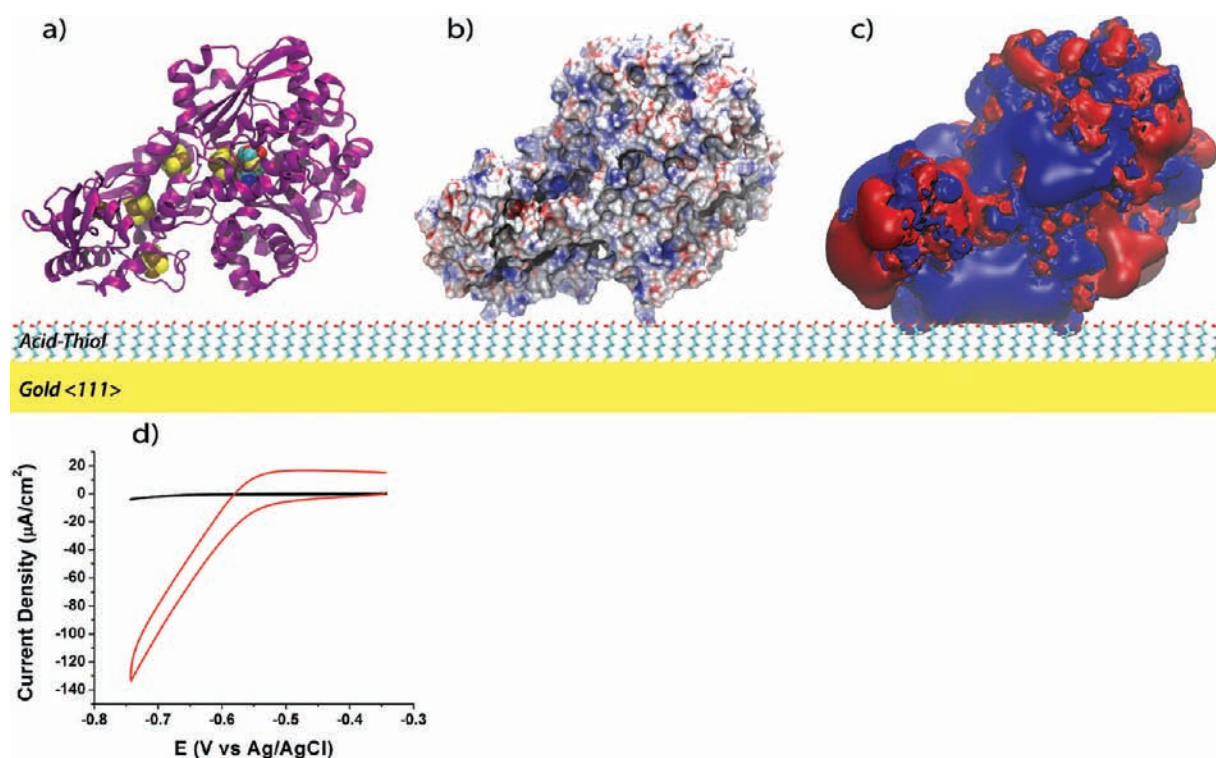


**Figure 1.** (a) Homology model of *CaHydA* [FeFe]-hydrogenase (see Supporting Information) on a 6-mercaptohexanoic acid-modified gold electrode. Panels a–c are shown for identical orientations. (b) Electrostatic surface potential of homology model of *CaHydA* on negatively charged SAM surface. (c) Isopotential surfaces generated by *CaHydA*. The +1 kcal/(mol·e) surface is depicted in blue, and the –1 kcal/(mol·e) surface is depicted in red. The orientation depicted in this panel maximizes the positive surface exposure to the carboxylates of the SAM, although other orientations are possible. (b, c) electrostatic calculations were performed at neutral pH and room temperature (25 °C). (d) Typical cyclic voltammogram of *CaHydA* on a 6-mercaptohexanoic acid-modified gold electrode. The black scan is a blank of the 6-mercaptohexanoic acid-modified electrode. The red scan depicts *CaHydA* adsorbed to the SAM.

adsorbed protein was consistent with *CaHydA* (see Supporting Information).

## RESULTS

**Assembly on SAMs.** SAMs were prepared on atomically flat gold electrodes with carboxylic-acid terminated alkanethiols. The acid moieties, which are negatively charged at the pH of these experiments, are designed to interact with the large regions of positive charge that are present on the protein surface. Ideally, such interactions are both strong and serve to orient the enzyme molecules all with the same face toward the gold. We employed SAMs having 3–11 carbon atoms in order to alter the distance between the protein and the electrode surface. Figure 1a–c depicts the proposed interaction between the positively charged protein surface and the negatively charged monolayer surface based on electrostatic considerations.<sup>39</sup> Although, the relative energies of this orientation and others were not rigorously calculated; the area of exposed positive charge of *CaHydA* interacting with the carboxylated surface of the SAM is maximized in these structures. Recently, Brown et al. have shown that CdTe nanocrystals capped with 3-mercaptopropionic acid interact with a region of positive charge on the surface of *CaHydA* to form a stable complex for the photoproduction of hydrogen.<sup>40</sup> Our system presumably utilizes the same region of positive charge, which surrounds the proposed binding site for the negatively charged ferredoxin during *in vivo* electron transfer.<sup>31</sup> This is the point where electrons are thought to enter the *CaHydA* electron

transfer chain. Cyclic voltammetric studies were performed on these Au-SAM electrodes with bound *CaHydA* and large catalytic electrochemical signals for hydrogen production were observed (Figure 1d), suggesting that the orientation of the protein on the electrode is favorable for electron transfer (ET).

**EC-STM.** EC-STM was chosen for imaging in this work for its ability to provide high-resolution imaging in a liquid medium as well as potentiostatic control of both tip and substrate. With *CaHydA* stably adsorbed onto carboxylate-terminated SAMs, the resulting surface was imaged, revealing random, relatively uniform coverage (Figure 2a–d). The electrochemical signal (Figure 1d) on the Au-SAM electrodes resembles that on PGE electrodes,<sup>10</sup> both in observed current density for short carbon chains, and waveform. It has been previously demonstrated that, under conditions like these, hydrogenase molecules free in solution do not contribute significantly to the catalytic current.<sup>30,41</sup> This suggests that the enzyme–surface interaction is stable and that the catalytic current can be ascribed to the enzyme molecules detected in the STM images.

The apparent height of the protein on the surface reflects the magnitude of the current flowing through the enzyme between the tip and gold substrate. This current changes with substrate potential (EC-STM) due to the properties of the redox active cofactors incorporated in the protein, specifically the distal [FeS] cluster which serves as an initial acceptor for intramolecular ET. As the substrate potential is shifted negative, the Fermi levels of both working electrodes (i.e., the tip and substrate) will bracket the redox level of the protein, at some point meeting resonant

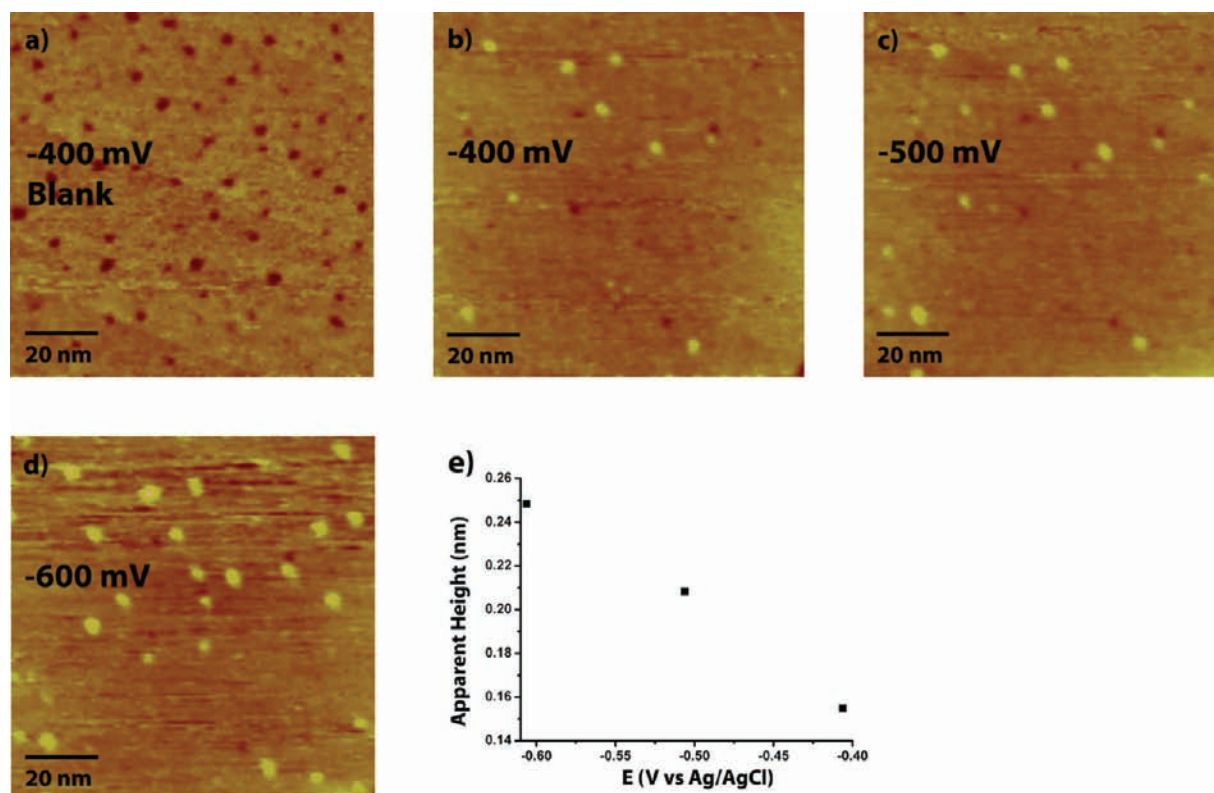


**Figure 2.** (a) EC-STM image of a 3-mercaptopropionic acid/ethanethiol SAM (1:1) on a Au (111) surface without protein;  $E_{\text{bias}} = 200$  mV,  $I_t = 400$  pA. (b–d) *CaHydA* adsorbed onto the modified surface at substrate potentials ranging from  $-400$  mV to  $-600$  mV vs Ag/AgCl. The images show an increasing apparent height with increasingly negative potentials. (e) Graph showing the apparent height of *CaHydA* as a function of potential.

tunneling conditions and giving rise to an increase in the tunneling current through the protein. A higher current is observed at roughly  $-0.6$  V vs Ag/AgCl, the potential at which proton reduction occurs, which is closely matched to the redox properties of the [FeS] clusters. Under these conditions, topographical STM images show larger apparent heights for the redox active hydrogenase (see Figure 2b–d). When the Fermi levels of the electrodes are positive or negative of the midpoint of the redox center (i.e., nonresonant tunneling conditions), the height appears smaller due to the decreased protein conductivity. Theoretically this observation should give a Gaussian distribution of heights versus substrate potential as the potential is swept past the midpoint of the redox center. This phenomenon has been recorded previously for redox proteins such as azurin<sup>42</sup> as well as other redox-active small molecules.<sup>43</sup> In our case, only one side of the curve can be observed due to limits imposed by solvent reduction at the tip at increasingly negative potentials.

**Cyclic Voltammetry.** The overall electrochemical properties of such electrodes may be studied using standard cyclic voltammetric techniques. A catalytic hydrogen production current due to enzymatic turnover is observed when sufficient driving force is applied to the electrode as seen in Figure 3a. For accurately measuring these currents, samples with high-density surface coverage ( $0.5$ – $2$  pmol/cm<sup>2</sup>) were prepared as seen in the inset of Figure 3a. The observed catalytic current is directly related to the amount of hydrogen produced from the enzyme. Taken together, the catalytic current and surface coverage (Figure 3a inset) were used for the calculation of a TOF per adsorbed *CaHydA*. The distance between the electrode and enzyme was altered by varying the SAM alkyl chain length from three to

eleven carbons. As a result, the current densities at a given voltage declined exponentially with increasing SAM length. Figure 3b depicts typical CVs of *CaHydA* on Au–SAM electrodes of lengths from three to eleven carbons, showing a decreasing catalytic current (i.e., turnover) for increasing chain length.

## DISCUSSION

From the catalytic hydrogen production current recorded through SAMs of various lengths and the number of enzyme molecules per electrode area counted from the STM images of each electrode, a TOF per molecule of *CaHydA* can be calculated at any given applied potential. The TOF per protein at  $-0.7$  V was plotted as a function of SAM length and fitted to an exponential decay function (Figure 3c) according to eq 1, where  $I$  is the tunnel current at a distance  $d$  from the electrode,  $I_0$  is the limiting current in the absence of the SAM layer, and  $\beta$  is the electronic decay constant.

$$I = I_0 e^{-\beta d} \quad (1)$$

An incremental distance per carbon in the alkyl chain of  $1.25$  Å was calculated on the basis of  $109.5^\circ$  carbon–carbon bond angles and a carbon–carbon bond length of  $1.54$  Å. From this, we calculated the length of the SAM alkyl chain and estimated the distance ( $d$ ) through which electron transfer between the enzyme surface and the electrode must occur. The experimental electronic decay constant was determined to be  $0.82 \pm 0.16$  Å<sup>-1</sup>. This agrees well with values reported in the literature for self-assembled monolayers of alkanethiols and is consistent with values obtained from drastically different techniques, including

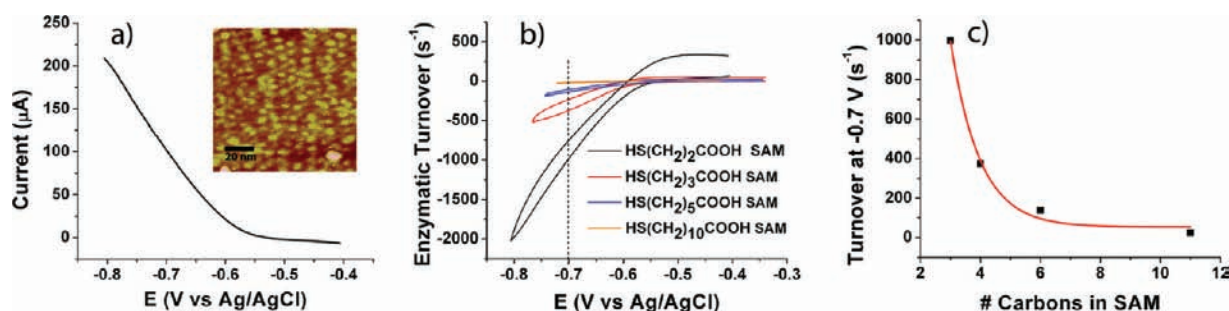


**Figure 3.** (a) Cathodic voltammogram of a high surface coverage *CaHydA* electrode. (Inset) STM image of the same electrode. Combining the voltammogram and protein coverage from the inset allows for calculation of a TOF per adsorbed protein molecule. (b) Enzymatic turnover of *CaHydA* recorded on different lengths of carboxylate-terminated SAMs as a function of applied potential. Rate data are determined for the cathodic scan at  $-0.7$  V vs Ag/AgCl, as indicated as a dashed line. (c) Single-protein turnover as a function of number of carbons in the SAM fit to an exponential function.

single-molecule junction measurements.<sup>44</sup> The exponential decay behavior is a consequence of control of the catalytic rate by ET through the SAM to the protein. ET through the protein itself to the catalytic site is the same for all SAM-protein constructs and, we conclude, does not control the catalytic rate at the potentials investigated.

Extrapolation of this plot to a distance of zero, approximating a *CaHydA* molecule in direct contact with the bare gold electrode surface where eq 1 simplifies to  $I = I_0$ , gave a TOF of  $\sim 21,000 \pm 12,000$  s<sup>-1</sup> at pH 7.0, which is higher than previous estimates in the literature for hydrogenases.<sup>11,28,29</sup> Methods using nonturnover signals for estimates of protein coverage have given a TOF upward of 10,000 s<sup>-1</sup>.<sup>4</sup> Catalytic current normalized by STM-derived surface density thus provides an average of the TOF for individual enzyme molecules for any given potential within the window of the electrochemical signal for *CaHydA*. This number does not account for inactive protein at the electrode interface or enzymes in an orientation unfavorable for interfacial ET and is thus a lower limit for turnover.

The electrochemical signal observed in cyclic voltammetry and the potential at which proton reduction occurs agree well with those reported in the literature for various electrode surfaces,<sup>10,17,20</sup> confirming that the kinetics of ET through the protein are not altered in this system. Theoretically, a limiting cathodic current should be observed when the rate of enzymatic proton reduction is slow compared to the rate of interfacial ET from the electrode to the protein. When these conditions are satisfied, the limiting current is directly related to the maximum turnover of the enzyme for the reduction of protons at a given pH. As the CVs indicate, even at the relatively low  $[H^+]$  used in our experiments, a limiting current was not observed. This may show that at these currents, a maximum turnover was not reached. There are other explanations for the observed lack of limiting currents. In one interpretation, a dispersion of nonspecific electrostatic protein–surface interactions (see Figure 1), such as could be the case with our system, preclude the direct observation of a limiting current.<sup>22</sup>

As a complement to the STM images, additional measures were taken to ensure the identity and quantity of *CaHydA*. To confirm the identity of the protein adsorbed to the surface, SDS-PAGE was run with samples recovered from the Au (111) substrates used for STM imaging experiments against purified *CaHydA*. Matching bands were observed at 65 kD (see Supporting Information). The detection of this small amount of protein was also consistent with the STM images in that three samples were combined for the SDS-PAGE, which was just sufficiently

above the limit of detection for visualization by silver staining.<sup>45–47</sup>

As an independent estimate of amount the *CaHydA* present on the STM substrate, samples were recovered under denaturing acidic conditions, and the Fe was quantified using a modified ferrozine assay.<sup>37,38</sup> Although this assay was near its limit of detection, the amount of Fe observed was also qualitatively consistent with the STM imaging results (see Supporting Information).

## CONCLUSION

We have designed a method for immobilizing an [FeFe]-hydrogenase, *CaHydA*, on an atomically flat gold electrode for topographic and electrochemical experiments on catalytically active samples. Direct observation of immobilized protein via EC-STM techniques shows the actual surface coverage which, when coupled with macroscopic electrochemical analysis, allows calculation of TOF as a function of potential at the single molecule level. From our analysis, we observe a TOF of  $\sim 1000$  s<sup>-1</sup> for *CaHydA* on a three-carbon SAM, and when extrapolated to bare gold, the TOF is estimated to be  $\sim 21,000$  s<sup>-1</sup> at  $-0.7$  V vs Ag/AgCl. Using a bipotentiostat, resonant tunneling at potentials consistent with the redox midpoints of cofactors within the protein was observed. The  $\beta$ -value of  $0.82 \text{ \AA}^{-1}$  for electron transfer through alkanethiol SAMs measured via determination of catalytic TOF is consistent with values obtained from radically different techniques, such as STM break junction. Taken together, the number of molecules calculated from the images, the exponential fit to the number of carbons in the SAMs, the value of  $\beta$ , and the indication of the redox activity for FeS centers form a consistent picture of electrocatalytic activity of *CaHydA* on SAMs. However, these results do not fully address the question of heterogeneity in the enzyme's catalytic activity or interaction with the electrode. The stability of immobilized *CaHydA* on SAMs under these conditions augurs well for future experiments to explore catalytic detail at the single molecule level.

## ASSOCIATED CONTENT

**S Supporting Information.** Extensive experimental details and CVs and STM images. This material is available free of charge via the Internet at <http://pubs.acs.org>.

## AUTHOR INFORMATION

**Corresponding Author**  
tmoore@asu.edu

## ■ ACKNOWLEDGMENT

We thank Professor Michael Hambourger for insightful discussions and helpful advice and Professor N. J. Tao for use of laboratory equipment. C.M. thanks Science Foundation Arizona for financial support. I.D.P. thanks the Marie-Curie International Outgoing Fellowship within the seventh European Community Framework and the MICINN Ramon y Cajal programs for financial support. M.V. is supported by the Graduate Research Fellowship Program from the National Science Foundation. K.A.B. and P.W.K. gratefully acknowledge funding by the U.S. Department of Energy, Division of Chemical Sciences, Geosciences, and Biosciences, Office of Basic Energy Sciences; and support by the U.S. Department of Energy under Contract No. DE-AC36-08-GO28308 with the National Renewable Energy Laboratory.

## ■ REFERENCES

- (1) Evans, D. J.; Pickett, C. J. *Chem. Soc. Rev.* **2003**, *32*, 268–275.
- (2) Armstrong, F. A. *Curr. Opin. Chem. Biol.* **2004**, *8*, 133–140.
- (3) Volbeda, A.; Fontecilla-Camps, J. C. *Coord. Chem. Rev.* **2005**, *249*, 1609–1619.
- (4) Vincent, K. A.; Parkin, A.; Armstrong, F. A. *Chem. Rev.* **2007**, *107*, 4366–4413.
- (5) Frey, M. *ChemBioChem* **2002**, *3*, 153–160.
- (6) Vincent, K. A.; Parkin, A.; Lenz, O.; Albracht, S. P. J.; Fontecilla-Camps, J. C.; Cammack, R.; Friedrich, B.; Armstrong, F. A. *J. Am. Chem. Soc.* **2005**, *127*, 18179–18189.
- (7) Parkin, A.; Cavazza, C.; Fontecilla-Camps, J. C.; Armstrong, F. A. *J. Am. Chem. Soc.* **2006**, *128*, 16808–16815.
- (8) Butt, J. N.; Filipiak, M.; Hagen, W. R. *Eur. J. Biochem.* **1997**, *245*, 116–122.
- (9) Goldet, G.; Brandmayr, C.; Stripp, S. T.; Happe, T.; Cavazza, C.; Fontecilla-Camps, J. C.; Armstrong, F. A. *J. Am. Chem. Soc.* **2009**, *131*, 14979–14989.
- (10) Hambourger, M.; Gervaldo, M.; Svedruzic, D.; King, P. W.; Gust, D.; Ghirardi, M.; Moore, A. L.; Moore, T. A. *J. Am. Chem. Soc.* **2008**, *130*, 2015–2022.
- (11) Jones, A. K.; Sillery, E.; Albracht, S. P. J.; Armstrong, F. A. *Chem. Commun.* **2002**, 866–867.
- (12) Alonso-Lomillo, M. A.; Rüdiger, O.; Maroto-Valiente, A.; Velez, M.; Rodríguez-Ramos, I.; Muñoz, F. J.; Fernández, V. M.; De Lacey, A. L. *Nano Lett.* **2007**, *7*, 1603–1608.
- (13) Guiral-Brugna, M.; Giudici-Ortoni, M. T.; Bruschi, M.; Bianco, P. J. *Electroanal. Chem.* **2001**, *510*, 136–143.
- (14) Lamle, S. E.; Vincent, K. A.; Halliwell, L. M.; Albracht, S. P. J.; Armstrong, F. A. *Dalton Trans.* **2003**, 4152–4157.
- (15) Johnston, W.; Cooney, M. J.; Liaw, B. Y.; Sapra, R.; Adams, M. W. W. *Enzyme Microb. Technol.* **2005**, *36*, 540–549.
- (16) Svedružić, D.; Blackburn, J. L.; Tenent, R. C.; Rocha, J.-D. R.; Vinzant, T. B.; Heben, M. J.; King, P. W. *J. Am. Chem. Soc.* **2011**, *133*, 4299–4306.
- (17) Krassen, H.; Stripp, S.; von Abendorth, G.; Ataka, K.; Happe, T.; Heberle, J. *J. Biotechnol.* **2009**, *142*, 3–9.
- (18) Hoeben, F. J. M.; Meijer, F. S.; Dekker, C.; Albracht, S. P. J.; Heering, H. A.; Lema, S. J. *ACS Nano* **2008**, *2*, 2497–2504.
- (19) Léger, C.; Bertrand, P. *Chem. Rev.* **2008**, *108*, 2379–2438.
- (20) Rüdiger, O.; Abad, J. M.; Hatchikian, E. C.; Fernandez, V. M.; De Lacey, A. L. *J. Am. Chem. Soc.* **2005**, *127*, 16008–16009.
- (21) Rüdiger, O.; Gutiérrez-Sánchez, C.; Olea, D.; Periera, I. A. C.; Velez, M.; Fernández, V. M.; De Lacey, A. L. *Electroanalysis* **2010**, *22*, 776–783.
- (22) Léger, C.; Jones, A. K.; Albracht, S. P. J.; Armstrong, F. A. *J. Phys. Chem. B* **2002**, *106*, 13058–13063.
- (23) Armstrong, F. A. *J. Chem. Soc., Dalton Trans.* **2002**, 661–671.
- (24) Heering, H. A.; Hirst, J.; Armstrong, F. A. *J. Phys. Chem. B* **1998**, *102*, 6889–6902.
- (25) Pershad, H. R.; Duff, J. L. C.; Heering, H. A.; Duin, E. C.; Albracht, S. P. J.; Armstrong, F. A. *Biochemistry* **1999**, *38*, 8992–8999.
- (26) Nakamura, C.; Mizutani, W.; Lantz, M. A.; Noda, K.; Zorin, N. A.; Miyake, J. *Supramol. Sci.* **1998**, *5*, 639–642.
- (27) Song, S.; Clark, R. A.; Bowden, E. F.; Tarlov, M. J. *J. Phys. Chem.* **1993**, *97*, 6564–6572.
- (28) Haas, A. S.; Pilloud, D. L.; Reddy, K. S.; Babcock, G. T.; Moser, C. C.; Blasie, J. K.; Dutton, P. L. *J. Phys. Chem. B* **2001**, *105*, 11351–11362.
- (29) Léger, C.; Dementin, S.; Bertrand, P.; Rousset, M.; Guigliarelli, B. *J. Am. Chem. Soc.* **2004**, *126*, 12162–12172.
- (30) Léger, C.; Jones, A. K.; Roseboom, W.; Albracht, S. P. J.; Armstrong, F. A. *Biochemistry* **2002**, *41*, 15736–15746.
- (31) King, P. W.; Posewitz, M. C.; Ghirardi, M. L.; Seibert, M. *J. Bacteriol.* **2006**, *188*, 2163–2172.
- (32) Peters, J. W.; Lanzilotta, W. N.; Lemon, B. J.; Seefeldt, L. C. *Science* **1998**, *282*, 1853–1858.
- (33) Pandey, A. S.; Harris, T. V.; Giles, L. J.; Peters, J. W.; Szilagy, R. K. *J. Am. Chem. Soc.* **2008**, *130*, 4533–4540.
- (34) Adams, M. W. W.; Mortenson, L. E. *J. Biol. Chem.* **1984**, *259*, 7045–7055.
- (35) Baffert, C.; Demuez, M.; Cournac, L.; Burlat, B.; Guigliarelli, B.; Bertrand, P.; Girbal, L.; Léger, C. *Angew. Chem., Int. Ed.* **2008**, *47*, 2052–2054.
- (36) Adams, M. W. W. *Biochim. Biophys. Acta* **1990**, *1020*, 115–145.
- (37) Stookey, L. L. *Anal. Chem.* **1971**, *42*, 779–781.
- (38) Carter, P. *Anal. Biochem.* **1970**, *40*, 450–458.
- (39) Kubiak-Ossowska, K.; Mulheran, P. A. *Langmuir* **2010**, *26*, 7690–7694.
- (40) Brown, K. A.; Dayal, S.; Ai, X.; Rumbles, G.; King, P. W. *J. Am. Chem. Soc.* **2010**, *132*, 9672–9680.
- (41) Bianco, P.; Haladjian, J. *J. Electrochem. Soc.* **1992**, *139*, 2428–2432.
- (42) Chi, Q.; Farver, O.; Ulstrup, J. *Proc. Nat. Acad. Sci. U.S.A.* **2005**, *102*, 16203–16208.
- (43) Tao, N. *J. Phys. Rev. Lett.* **1996**, *76*, 4066–4069.
- (44) Cui, X. D.; Zarate, X.; Tomfohr, J.; Sankey, O. F.; Primak, A.; Moore, A. L.; Moore, T. A.; Gust, D.; Harris, G.; Lindsay, S. M. *Nanotechnology* **2002**, *13*, 5–14.
- (45) Schägger, H.; von Jagow, G. *Anal. Biochem.* **1987**, *166*, 368–379.
- (46) Schägger, H. *Nat. Protoc.* **2006**, *1*, 16–22.
- (47) Winkler, C.; Denker, K.; Wortelkamp, S.; Sickmann, A. *Electrophoresis* **2007**, *28*, 2095–2099.